Innovative therapeutic strategies for intrauterine adhesions: Role of umbilical cord mesenchymal stem cells in rat models

MINGLE ZHANG[1,2], HE GAO[1,2], JIAHUA ZHENG[1,2], YANFAN DU[1,2], YANPENG TIAN[3], YANLAI XIAO[1,2], QIAN LI[1,2], ZHONGKANG LI[1,2] and XIANGHUA HUANG[1,2]

[1]Department of Gynecology, The Second Hospital of Hebei Medical University, Shijiazhuang, Hebei 050000, P.R. China; [2]Hebei Key Laboratory of Regenerative Medicine of Obstetrics and Gynecology, The Second Hospital of Hebei Medical University, Hebei Provincial Department of Science and Technology, Shijiazhuang, Hebei 050000, P.R. China; [3]Department of Obstetrics and Gynecology, The First Affiliated Hospital of Zhengzhou University, Zhengzhou, Henan 450000, P.R. China

Received July 16, 2024; Accepted November 15, 2024

DOI: 10.3892/etm.2025.12805

Abstract. Intrauterine adhesions (IUAs) represent a considerable impediment to female reproductive health. Despite ongoing debate regarding the optimally efficacious route of administration and dosage of stem cells for IUA treatment, human umbilical cord-derived mesenchymal stem cells (UCMSCs) have emerged as a promising avenue for regenerative therapy. The present study aimed to investigate the potential effects of UCMSCs on IUAs and to further explore the most effective treatment route and dosages. In the present study, the therapeutic potential of UCMSCs in a constructed rat model of IUAs was evaluated. The efficacy of UCMSC administration through three different routes, namely intraperitoneal injection, in-site injection and caudal vein injection, was compared at three different doses of cells ($0.5x10^6$, $1x10^6$ and $5x10^6$). The assessment parameters included endometrial thickness, glandular density and extent of fibrotic tissue, which were measured using HE staining and Masson staining and numbers of offspring. The IUA model group compared with the control group endometrial thickness decreased, glandular density decreased and the extent of fibrotic tissue increased, suggesting the IUA rat model had been successfully established. At 4 weeks post-treatment, an intraperitoneal injection of $1x10^6$ UCMSCs (the middle dose) was found to have led to a significant increase in endometrial thickness and glandular count, approaching the levels that were observed in the normal group. This dosage also notably reduced the level of fibrosis compared with that in both the higher and the lower doses, although this remained slightly higher compared with that observed in the normal group. Furthermore, the reproductive capability of the rats in the higher and middle dosage IUA rat model exhibited partial recovery post-treatment. In conclusion, the results of the present study suggest that the intraperitoneal administration of $1x10^6$ UCMSCs can provide a viable strategy for promoting endometrial regeneration and reducing fibrosis in IUA. In addition, this highlights the potential of UCMSC therapy as a means of clinical intervention for severe IUA, ultimately improving fertility outcomes, especially with regard to the specific dosage and intraperitoneal injection method.

Correspondence to: Professor Xianghua Huang or Dr Zhongkang Li, Department of Gynecology, The Second Hospital of Hebei Medical University, 215 Heping West Road, Shijiazhuang, Hebei 050000, P.R. China
E-mail: huangxh2022@hebmu.edu.cn
E-mail: zhongkangli@hebmu.edu.cn

Key words: intrauterine adhesions, umbilical cord-derived mesenchymal stem cells, fibrosis reduction, reproduction, regenerative medicine

Introduction

Intrauterine adhesions (IUAs), characterized by fibrous scar formation within the uterine cavity, pose a significant clinical challenge due to their adverse effects on female fertility (1). Predominantly associated with post-surgical traumas, especially following various procedures, such as dilatation and curettage, the prevalence of IUAs varies based on the extent and frequency of uterine surgeries (2). These adhesions contribute to various reproductive dysfunctions, including menstrual irregularities, reduced fertility, recurrent miscarriages and placental abnormalities (3). Current treatment strategies mainly involve surgical interventions, most notably hysteroscopic adhesiolysis, which is frequently combined with hormonal therapies to promote endometrial regeneration (1). Although these approaches are able to restore the uterine anatomy and improve menstrual outcomes to a certain extent, their long-term efficacy in preserving reproductive function is limited due to high recurrence rates and adhesion reformation (4). In addition, the invasive nature of these treatments predisposes patients to further risks of adhesion development (3), highlighting the urgent need to develop novel therapeutic strategies that are both less invasive and more effective in restoring complete reproductive potential.

Advances in regenerative medicine have prominently featured mesenchymal stem cells (MSCs) as potential agents for tissue repair and functional restoration across a broad spectrum of organ systems (5,6). Amongst the various MSC sources,

umbilical cord-derived MSCs (UCMSCs) are distinguished by their superior proliferation rates, robust differentiation capabilities and reduced immunogenicity compared with MSCs harvested from adult tissues (7). These attributes render UCMSCs suitable as clinical tools aimed at repairing organ damage (8). Previous *in vitro* studies have demonstrated that UCMSCs are able to significantly enhance the proliferation of damaged endometrial stromal cells and upregulate the expression of vascular angiogenesis markers (9,10). Furthermore, in animal models, UCMSCs have been reported to repair endometrial injury, restore fertility, and promote endometrial cell proliferation and vascular remodeling (11,12). Other preliminary studies have also demonstrated that UCMSCs can effectively promote endometrial regeneration and attenuate fibrosis in rhesus monkeys with intrauterine adhesion models, indicating their potential applicability for human therapies (13). However, in reproductive medicine, the application of UCMSCs for treating IUAs remains in developmental stages.

Although UCMSCs have demonstrated promise in regenerative medicine, their use in treating IUAs is confronted with a number of unresolved issues. The optimal dosage and delivery route for UCMSCs therapy remain to be determined. Various methods that have been attempted, such as intraperitoneal, intrauterine and intravenous injections, have shown mixed results in terms of cell engraftment and efficacy (14). Additionally, concerns persist regarding potential immune responses, insufficient cell retention, and the long-term safety and durability of treatment efficacy (15). To the best of our knowledge, the majority of studies of using UCMSCs for the treatment of IUA to date have been performed on animal models, where the translational possibility of these findings to the clinic have not been explored. Therefore, the present study aimed to address these challenges by systematically evaluating different UCMSC doses and administration routes in a rat model of IUA, focusing on endometrial regeneration, fibrosis, and immune responses, to provide insights for the optimization of stem cell therapies for IUA.

The present study investigated the therapeutic potential of UCMSCs for treating IUAs using a rat model. Through systematically comparing different administration routes and dosages, the aim is to optimize the delivery method for enhancing endometrial repair and reducing fibrosis.

Materials and methods

Isolation, cultivation and identification of UCMSCs. UCMSCs were isolated from fresh, full-term umbilical cords of women who gave birth at term in The Second Hospital of Hebei Medical University (Shijiazhuang, China) from January 2021 to December 2022 were collected, and informed consent was obtained from the six mothers who donated the umbilical cords for research purposes (n=6; mean age, 35.83±3.061 years), with each mother providing one umbilical cord. The inclusion criteria were: Healthy mothers with full-term deliveries. The exclusion criteria were: Mothers with pregnancy complications or pre-existing medical conditions, and those whose fetuses were diagnosed with developmental abnormalities during prenatal screening. The present study was approved by the Ethical Committee of the Second Hospital of Hebei Medical University (Shijiazhuang, China; approval no. 2020-R285). The cords were first washed with PBS supplemented with an antibiotic/antimycotic solution to mitigate microbial contamination. Subsequently, Wharton's jelly was dissected from the cords and cut into small explants of 1-2 cm^3. These explants were then placed onto culture dishes pre-coated with 0.1% gelatin (HapCult™; Precision BioMedicals Co., Ltd.) to enhance cell adhesion, before the plates were cultured in DMEM (Gibco; Thermo Fisher Scientific, Inc.) enriched with 10% FBS (Gibco; Thermo Fisher Scientific, Inc.), 1% L-glutamine (Gibco; Thermo Fisher Scientific, Inc.) and 1% penicillin and streptomycin solution (Gibco; Thermo Fisher Scientific, Inc.) at 37˚C in an atmosphere containing 95% air/5% CO_2. The medium was initially replaced after 72 h to eliminate non-adherent cells, and then replaced every 3 days. Once the cells had reached 80-90% confluence, they were detached using 0.25% trypsin-EDTA (Gibco; Thermo Fisher Scientific, Inc.) and subsequently passaged. Cells at passages 3-7 were utilized for further experiments to ensure consistency and vitality. The morphological features of UCMSCs were continuously monitored under an inverted light microscope (Carl Zeiss AG), where they displayed a typical fibroblast-like morphology.

The UCMSCs were identified as previously described (16). Cells were first observed under an inverted light microscope to confirm their morphology. Subsequently, phenotypic characterization was performed using flow cytometric (FCM) analysis with a BD FACSCanto™ II flow cytometer (BD Biosciences). Cells were stained with fluorescently labeled antibodies to confirm their mesenchymal lineage, whereas hematopoietic elements were excluded. Additionally, H&E staining was performed on cellular smears to further authenticate their morphology.

FCM analysis. FCM analysis was performed to phenotypically identify the UCMSCs. Cells were detached using 0.25% trypsin-EDTA, after adding trypsin and incubating at room temperature for 1-3 min, PBS containing 2% FBS was added and stained with fluorescently labeled antibodies against MSC markers CD90-FITC (1:400; cat. no. 555595), CD44-PE (1:400; cat. no. 566803), CD105-PerCP (1:400; cat. no. 323215), CD73 PE (1:400; cat. no. 550257) and CD29-APC (1:400; cat. no. 559883) (all purchased from Biolegend, Inc.) and negative markers human leukocyte antigen (HLA)-DR-APC (1:400; cat. no. 307609) and CD45-FITC (1:400; cat. no. 555488) (both from BioLegend, Inc.). The number of cells per aliquot for antibody staining ranged from $5x10^6$ to $10x10^6$ cells. Following a 30-min incubation at 4˚C, the cells were washed, fixed in 1% paraformaldehyde at room temperature for 10-15 min. If prompt analysis on the machine was not feasible, fixation was required, followed by storage at 4˚C in the dark. Analysis was conducted within 24 h. If analysis was performed immediately, the fixation step was unnecessary (fixed with 1% paraformaldehyde at room temperature for 10-15 min). After antibody labeling, the cells were incubated at room temperature in the dark for 15 min. Subsequently, 1 ml of PBS was added to wash the cells. The cells were then centrifuged at 300 x g for 5 min at 4˚C, and the supernatant was discarded. Finally, the cells were resuspended in 500 to 1,000 μl of PBS and analyzed using flow cytometry (CellQuest; BD Biosciences). Data obtained

from ≥10,000 events per sample confirmed a high expression level of mesenchymal markers and a low expression level of hematopoietic markers, verifying their MSC identity.

CM-Dil labeling of UCMSCs. To track the cellular integration of UCMSC post-transplantation, CellTracker™ CM-DiI dye (cat. no. C7000; Life Technologies; Thermo Fisher Scientific, Inc.), a lipophilic fluorescent dye, was used for staining the cell membranes. The passage 3 UCMSCs were first incubated with the CM-Dil solution (the CM-Dil working solution was prepared in advance for fluorescence staining using a ratio of CM-Dil stock solution to medium of 1:1,000). Following an incubation at 37˚C in an atmosphere containing 5% CO_2 for a predetermined duration, the cells were washed with PBS to remove the excess dye. Successful dye incorporation was verified under a fluorescence microscope, with cell nuclei counterstained using DAPI at room temperature 5 min (cat. no. 0100-20; SouthernBiotech) to enhance visualization.

Animal experiment and construction of the IUA model. All animals were housed in a pathogen-free facility at the Animal Center of the Second Hospital of Hebei Medical University. The rats were kept in standard cages under controlled conditions (12-h light/dark cycle, temperature of 22-24˚C and 40-60% humidity) with *ad libitum* access to food and water. Humane endpoints were predefined to minimize animal suffering. Rats exhibiting signs of distress, severe illness or immobility were humanely euthanized using an overdose of pentobarbital sodium (100 mg/kg, intraperitoneal injection). The total duration of the experiment was 18 weeks, which included a 2-week post-modeling period for IUA induction, and 4 weeks of treatment and observation following UCMSC administration, followed by 12 weeks of the co-housing experiment. A total of 174 rats (149 female rats and 25 male rats) were used in the present study. All animals were humanely euthanized at the conclusion of the experiment. No animals reached the humane endpoint and no animals were found dead during the experiments.

The IUA model was established using female Sprague-Dawley (SD) rats, aged 6-8 weeks and weighing between 180-220 g, which were procured from the Hebei Medical University Animal Experiment Center. All animal experiments were conducted with approval from the Ethical Committee of the Second Hospital of Hebei Medical University (approval no. 2021-AE261). A total of 12 rats were randomly divided into two groups: A normal control group (n=6 rats) and a model group (n=6 rats). The use of 6 rats in the modeling group was based on previous studies and statistical power analysis that indicated this number to be sufficient for histological assessments (17). In similar studies, a sample size of 6 has been shown to provide reliable and reproducible data for evaluating tissue morphology and fibrosis (18).

The IUA model in the present study was based on a dual-injury approach: Mechanical injury (scratching) combined with lipopolysaccharide (LPS) application. The primary focus was on mechanical injury, with LPS used to represent secondary infection, which can occur following intrauterine procedures and may contribute to adhesion formation (17-19). This method was chosen to reflect clinical situations where infection may serve a role in adhesion development after surgical interventions.

The rat model of IUA was established following previously reported protocols (17-19). To quantify the migration of CM-Dil-labeled UCMSCs to the dual-injured uterus in SD rats, the following procedure was performed. Briefly, SD rats were anesthetized using an intraperitoneal injection of sodium pentobarbital at a dose of 40 mg/kg body weight and subjected to a midline abdominal incision (2-2.5 cm). The endometrial lining was then scraped using a 2.5-mm endometrial curette (RWD Life Science Co., Ltd.) until the uterine wall became visibly rough. LPS-coated sutures were subsequently placed into the cavity of one uterine horn, with one end fixed to the skin through the muscle layer. The sutures were removed after 48 h. Model stability was confirmed after three estrous cycles. Our previous research conducted observations at 1, 2, 4, 8 and 12 weeks after IUA modeling. When comparing the 2-week post-modeling period with 4, 8 and 12 weeks, there were no significant changes in endometrial thickness, glandular density, and extent of fibrotic tissue (17). Our research team (17-19) used the same IUA modeling method and confirmed that the 2-week IUA model reached a stable state. CM-Dil-labeled UCMSCs were injected into the abdominal cavity, tail vein, and uterine myometrium. The animals were euthanized on days 3, 7 and 14 post-transplantation, and the uteri were subjected to rapid frozen sectioning followed by immunofluorescence tracing. In the present study, the time points for euthanasia varied depending on the experimental purpose. During the fluorescent tracing experiment, rats were euthanized at D3, D7 and D14 to track the distribution and persistence of the transplanted cells over time. By contrast, for the stem cell treatment experiment, rats were euthanized only at D28 to perform histological analyses and evaluate the therapeutic effects of stem cell therapy on uterine tissues. Thus, D3, D7 and D14 were specifically used to investigate the localization of the transplanted stem cells, while D28 was used to assess the outcomes of the treatment.

Analysis of the effects of UCMSC administration routes on IUA treatment. Female SD rats were categorized into five groups, each comprising 6 animals for histological examination and 5 animals for fertility testing (totaling 11 rats in each group; Table I), to assess the impact of different UCMSC administration routes on IUA. The groups included the following: i) A normal group (Normal), with no modeling or treatment; ii) a model group (IUA group), in which the rats underwent IUA modeling without any treatment; iii) an intraperitoneal injection group (IP group), in which the rats received UCMSCs through intraperitoneal injection after IUA modeling; iv) an in-site injection group (IS group), where the rats were treated with UCMSCs directly into the intrauterine wall post-modeling; and v) an injection of caudal vein group (IOCV group), where the rats were administered UCMSCs through the tail vein following IUA induction.

To ascertain the therapeutic efficacy of UCMSCs on IUA, UCMSCs were administered to female SD rats through the three distinct routes (intraperitoneal injection, in-site injection and caudal vein injection), where each rat received a standardized dose of 1x106 cells. Over a 4-week post-transplantation period, the health of the rats was monitored, with particular

Table I. Experimental grouping for UCMSC administration.

A, Phase 1: Administration route

Group	Total rats, n	Histological analysis, n	Fertility testing, n
Normal group	11	6	5
Model group	11	6	5
Intraperitoneal injection group	11	6	5
In site injection group	11	6	5
Intravenous injection group	11	6	5

B, Phase 2: Dosage validation

Group	Total rats, n	Histological analysis, n	Fertility testing, n
Normal group	11	6	5
Model group	11	6	5
Low dose ($0.5x10^6$ UCMSCs)	11	6	5
Medium dose ($1x10^6$ UCMSCs)	11	6	5
High dose ($5x10^6$ UCMSCs)	11	6	5

A total of 174 rats were used in this study. The table shows the grouping information for 162 of these animals. An additional 12 rats were used for model induction, which are not included in the table. UCMSCs, human umbilical cord-derived mesenchymal stem cells.

attention given to any adverse reactions or complications. At the end of the observation period (D28), all animals were euthanized via intraperitoneal injection of an overdose of sodium pentobarbital (100 mg/kg). Death was confirmed by the cessation of heartbeat and pupil dilation. The uteri were subsequently collected for comprehensive histopathological evaluation. Histological assessments were performed using H&E and Masson's trichrome staining to evaluate endometrial regeneration and fibrosis. Quantitative analyses of endometrial thickness, gland density and fibrotic areas were performed using ImageJ software (Image J 1.53e. Java 1.8.0_172; National Institutes of Health), and immune responses were assessed by measuring serum IgG levels using ELISA.

Intraperitoneal administration of UCMSCs at various concentrations for treating IUAs. To investigate the effect of different concentrations of intraperitoneally administered UCMSCs on the treatment efficacy for IUA, three dosage groups were established among the model rats: A low-dose group (with the administration of $0.5x10^6$ cells), a medium-dose group (receiving $1x10^6$ cells) and a high-dose group (treated with $5.0x10^6$ cells). The dosage selection was based on preliminary experiments that were conducted to identify the most appropriate and effective dosage range for treatment (17), ensuring the doses used were within the therapeutic window. The normal group underwent a sham operation (abdominal incision without injury, no IUA induction, and no stem cell treatment) and served as the baseline control. The model group received the IUA induction without stem cell treatment, providing a reference for evaluating the effects of UCMSC therapy. Each group consisted of 11 rats (6 for histological assessment and 5 for mating experiments; Table I), all of which had undergone IUA induction and received UCMSC administration through the route of intraperitoneal injection. After 4 weeks of monitoring the rats for adverse effects, they were euthanized and uterine tissue samples were collected. Histological assessment was subsequently performed as previously described in analysis of the effects of UCMSC administration routes on IUA treatment.

Assessment of fertility restoration post-treatment with UCMSCs. To assess the efficacy of UCMSCs on fertility after IUA, a cohabitation study was initiated after the initial 4-week treatment period. In total, 5 female Sprague-Dawley rats from each experimental group were randomly selected and paired with fertile male rats at a 1:1 ratio. The pairs were housed under controlled environmental conditions (temperature, 20-25˚C; humidity maintained at 50-60%; and the light/dark cycle of 12 h of light followed by 12 h of darkness) optimal for breeding for a duration of 12 weeks, with food and water provided *ad libitum*. The mating pairs were observed daily to monitor for signs of pregnancy, which were initially indicated by physical changes in the females and subsequently confirmed through palpation. Post-gestation, the number of offspring for each female was recorded. No offspring were sacrificed in this study. Instead, these offspring were donated to the Hebei Medical University Animal Experiment Center for use in other research projects. These data served as a direct indicator of the fertility potential of UCMSC treatment, providing insights into the success rate and possible enhancements in reproductive health, of the rats following the intervention for IUAs.

H&E staining. H&E staining was used to assess morphological changes in the uterine tissue post-treatment. Samples were fixed in 4% neutral buffered formalin at room temperature for 24 h, dehydrated in an ascending ethanol gradient, cleared in

xylene and paraffin-embedded. Sections of 5 μm in thickness were deparaffinized, rehydrated and stained with hematoxylin for nuclei (at room temperature for 30 min) and counterstained with eosin (at room temperature for 30 sec) for cytoplasmic and extracellular components. The slides were subsequently dehydrated, cleared and mounted in a xylene-based medium. Microscopic examinations at magnifications of x100, x200 and x400 were undertaken to evaluate the endometrial thickness, cellular integrity and extent of fibrosis. Endometrial thickness was measured using H&E-stained sections imaged under a low-power light microscope. In total, four perpendicular points were selected within each section and the thickness was measured at these points. The average of these measurements was calculated to determine the final endometrial thickness. Finally, images were taken for comparative analysis among the experimental groups.

Masson's trichrome staining. Masson's trichrome staining was used to assess the extent of fibrosis in the uterine tissues post-UCMSC treatment. Tissue sections, embedded in paraffin and sliced to a thickness of 5 μm, underwent deparaffinization in xylene and rehydration through a descending graded alcohol series. Staining involved the sequential application of Weigert's iron hematoxylin for 7 min, Biebrich scarlet-acid fuchsin for 15 min, and aniline blue for 2 min, and all procedures were completed at room temperature. Quantitative fibrosis analysis was performed using image processing software (Image J 1.53e. Java 1.8.0_172; National Institutes of Health) to measure fibrosis area and intensity in four randomly selected fields of view.

ELISA. To assess the immunological response following transplantation of the UCMSCs, the serum IgG levels were measured using ELISA. Blood samples (1 ml per rat) were collected from the tail vein immediately prior to euthanasia after the 4-week treatment period and the serum was separated by centrifugation at 3,018.6 g for 15 min at room temperature, before being stored at -20˚C for analysis. Using a specific Rat IgG ELISA kit (cat. nos.866, Meimian Technology Co., Ltd.) for IgG according to the manufacturer's instructions, 100 μl serum was added to anti-rat IgG-coated wells on a 96-well plate. After incubating and washing the plate, an HRP-conjugated secondary antibody was used to detect bound IgG. The reaction was developed with tetramethylbenzidine and stopped by the addition of sulfuric acid. The optical density was subsequently measured at 450 nm using a microplate reader and the IgG levels were quantified against a standard curve.

Statistical analysis. Each experiment was performed at least three times. Statistical analysis was performed using SPSS version 26.0 (IBM Corp.). Continuous variables were presented as mean ± standard deviation. One-way ANOVA was used for the homogeneous variance in ≥3 group comparisons followed by the Tukey's test for multiple comparisons between groups. Welch's ANOVA was applied to the uneven variance in ≥3 group comparisons followed by the Games-Howell method between groups. $P<0.05$ was considered to indicate a statistically significant difference. Each data analysis included at least three independent molecular experiments, with a minimum of three animal samples per group in each experiment.

Results

Isolation, cultivation and characterization of UCMSCs. After the UCMSCs had been successfully isolated and cultured within ~2 weeks, spindle-shaped cells began to migrate from the explanted tissue pieces and reached 80-90% confluence, displaying a characteristic 'whirlpool-like' pattern in their arrangement (Fig. 1A). Further phenotypic characterization through FCM analysis confirmed the mesenchymal identity of the cells. Specifically, the cells were found to exhibit high expression levels of MSC markers CD90, CD44, CD105, CD73 and CD29, with minimal expression of the hematopoietic markers HLA-DR and CD45, thereby validating their mesenchymal lineage from Wharton's jelly (Fig. 1B). Subsequently, the morphological characteristics of the UCMSCs were assessed using H&E staining, which revealed elongated, spindle-shaped cells with well-defined oval nuclei and light red cytoplasm, exhibiting a uniform fusiform shape, growing in a vortex-like or parallel pattern, and arranged in a neat and orderly fashion adherent to the substrate (Fig. 1C). These results confirmed the successful isolation and characterization of UCMSCs, where the specific marker profile supported their identity as MSCs.

CM-Dil labeling and in vivo tracking of UCMSCs. Post-transplantation tracking of UCMSCs was achieved using CM-Dil. After completion of the labeling process, UCMSCs exhibited strong red fluorescence in the cytoplasm, confirming successful uptake of the dye. Their nuclei were counterstained with DAPI, producing a striking blue fluorescence (Fig. 1D). This dual-color imaging process enabled precise tracking of the UCMSCs in the rat IUA model, confirming that the CM-Dil-labeled cells both maintained their structural integrity and were easily identifiable within the target tissues.

The localization and persistence of UCMSCs within rat uterine tissues were tracked using fluorescence imaging following transplantation. Fig. 2 specifically shows the distribution of UCMSCs post-transplantation and does not include data from IUA-induced rats or a normal control group. The figure was designed solely to evaluate the *in vivo* localization of the transplanted cells. Cells were pre-labeled with a fluorescent dye for enhanced visualization in the tissue sections. By day 3, fluorescently labeled UCMSCs were detectable in all treatment groups, confirming successful engraftment (Fig. 2). By day 7, the IP group exhibited widespread fluorescence throughout the uterine muscular and interstitial tissues, whereas the IS group exhibited no detectable fluorescence in the muscular layer, indicating poor retention. The IOCV group displayed localized fluorescence at the endometrial-myometrial junction, indicating route-specific migration patterns. By day 14, all experimental groups exhibited fluorescent markers near the uterine cavity's inner lining, suggesting retention and potential integration of UCMSCs into the endometrial layer (Fig. 2).

Construction of the rat IUA model. Following the established modeling procedures, a rat model of IUA was developed (Fig. 3A-D). Histological analysis using H&E staining revealed a significant reduction in the endometrial

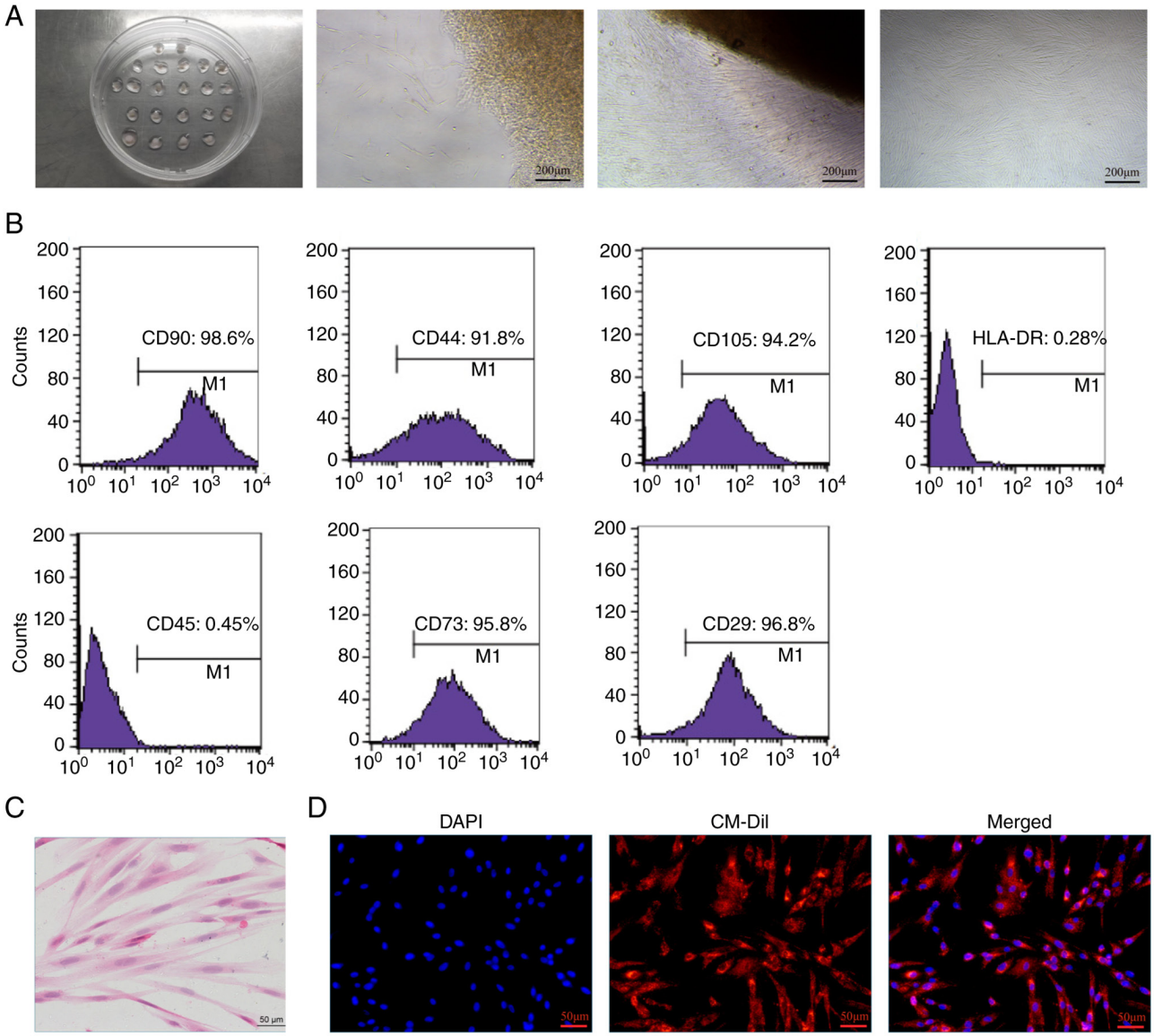

Figure 1. Isolation and characterization of UCMSCs. (A) Representative images of the culture process, showing the progression from explanted tissue pieces to 80-90% confluence of spindle-shaped cells with a characteristic 'whirlpool-like' arrangement. From left to right: Tissue-culture plate, initial tissue adhesion, early cell migration and near-confluent culture. (B) Flow cytometry histograms, demonstrating the expression of mesenchymal stem cell markers (CD90, CD44, CD105, CD73 and CD29) and minimal expression of hematopoietic markers (HLA-DR and CD45). Each panel shows the percentage of cells expressing the respective marker, confirming the mesenchymal phenotype. (C) H&E-stained micrograph of UCMSCs, highlighting elongated, spindle-shaped cells with well-defined, oval nuclei and light red cytoplasm. (D) Fluorescence microscopy images of UCMSCs stained with DAPI (blue) for nuclei, CM-Dil (red) for cell membranes and a merged image showing the co-localization of DAPI and CM-Dil, illustrating cell morphology and integrity. The scale bar represents 50 μm. The data shown are representative of three independent experiments (each data analysis included at least three independent molecular experiments, with a minimum of three animal samples per group in each experiment). UCMSCs, human umbilical cord-derived mesenchymal stem cells.

thickness in the model group compared with that in the normal group (P<0.05; Fig. 3E and Table II). The number of endometrial glands also decreased significantly in the model group compared with that in the normal group (P<0.05), suggesting the occurrence of substantial glandular loss due to induced adhesions (Fig. 3E and Table II). Furthermore, the Masson's trichrome staining experiments demonstrated a significant increase in fibrotic areas within the endometrial interstitium of the model group compared with that in the normal group (P<0.05; Fig. 3E and Table II). Collectively, these data suggest the efficacy of the combined mechanical and infection-induced injury methods in replicating IUAs in rats.

Effects of different UCMSC administration routes on IUA treatment. The effectiveness of the different administration routes of UCMSCs that were investigated in the present study in terms of treating IUAs was evaluated through various histological and immunological assessments. Significant differences in endometrial thickness and gland numbers were observed comparing among the experimental groups (P<0.001 for thickness; P<0.001 for gland number; Fig. 4A, C and D). In particular, the IP group demonstrated an increase in endometrial thickness, which was around normal levels and was significantly higher compared with that in the IS and IOCV groups. Additionally, the gland density was also higher in the IP group (close to normal)

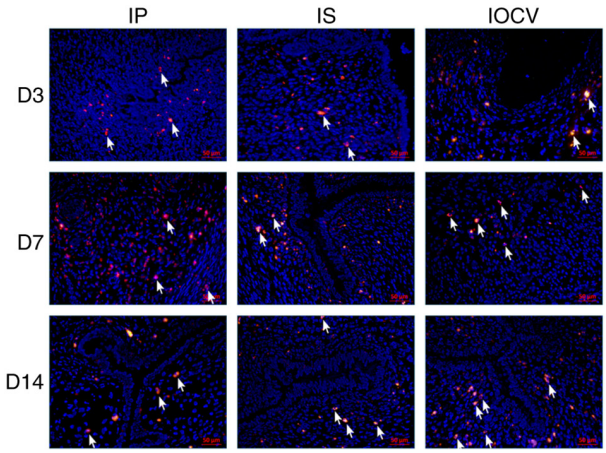

Figure 2. Localization and dynamics of human umbilical cord-derived MSCs in rat uterine tissues following transplantation. D3: Early engraftment of fluorescently labeled MSCs (red) with nuclear staining (blue) in all treatment groups. D7: Diverse patterns of cell persistence: Widespread in the IP group, minimal in the IS group and localized at the endometrial-myometrial junction in the IOCV group. D14: Enhanced accumulation near the inner lining of the uterine cavity, suggesting potential integration into the endometrial layer. White arrows indicate initial cell localization. Scale bars, 50 μm. Data are representative of three independent experiments, with three rats per group. D, day; MSCs, mesenchymal stem cells; IP, intraperitoneal; IS, intrauterine site injection; IOCV, intravenous ovary-cervix.

compared with that in the IS group and the baseline IUA model.

The extent of fibrosis was also shown to be significantly different among the experimental groups (P<0.001), with the IP group showing the lowest percentage of fibrotic areas, a value that was significantly lower compared with that in the IS, IOCV and IUA groups (Fig. 4B and E). IgG levels, measured using ELISA, showed an initial rise within 3-7 days post-transplantation in the five groups, although this trend was followed by diverging trends afterwards. The IP group exhibited a rapid increase in IgG levels, which were later stabilized, whereas the IS and IOCV groups exhibited a more gradual increase (Fig. 4F). By day 28, the normal group had the lowest immune response, whereas the IOCV group showed markedly higher levels, reflecting the varying immunological impacts of the different treatments. Taken together, these findings underscored the distinct impact of different UCMSC administration routes on both structural restoration and the immunological environment in the IUA model of rats.

Effects of different concentrations of UCMSCs administered intraperitoneally on IUA treatment. This series of experiments assessed the therapeutic efficacy of administering different concentrations of UCMSCs intraperitoneally in a rat model of IUA. Specifically, significant differences in endometrial thickness were observed among the five groups (P<0.001; Fig. 5A and C). The group treated with 1.0x10^6 UCMSCs (the middle dose) exhibited a substantial increase in thickness, surpassing the low-dose (0.5x10^6 cells) and high-dose (5.0x10^6 cells) groups, where the thickness was comparable with that of the normal group, indicating effective endometrial regeneration. Gland numbers also varied significantly (P<0.001; Fig. 5A and D). The 5.0x10^6 cells treatment group exhibited a significantly higher gland count compared with that in the 0.5x10^6 cells treatment group and the baseline IUA model, which was comparable with the normal and 1.0x10^6 cells groups, suggesting a dose-dependent effect on glandular restoration. The differences in fibrotic area were also found to be statistically significant (P<0.001; Fig. 5B and E). The 1.0x10^6 cells (middle dose) group exhibited the lowest fibrotic percentage, which was significantly lower compared with that in the high dose, low dose and the baseline IUA model groups, highlighting the optimal dose for minimizing fibrosis. Taken together, these findings suggested that the concentration of UCMSCs that is administered intraperitoneally critically influences both endometrial tissue regeneration and fibrosis reduction.

Table II. Assessment of the stability of the intrauterine adhesion model.

Parameters	Glands, n	Thickness, μm	Fibrotic area, %
Normal	25.7±5.3	612.1±41.3	19.9±1.5
Model	11.8±5.2	413.8±115.2	50.5±11.3
P-value	0.001	0.005	0.001

Assessment of fertility post-UCMSC treatment. Subsequently, the fertility restoration capabilities of various concentrations and administration routes of UCMSCs were next systematically evaluated. A 12-week co-housing experiment was performed to assess the reproductive outcomes by counting the offspring from different treatment and control groups (Fig. 6A). No pregnancies were observed in the IUA model group (Fig. 6B) or the low-dose UCMSC (0.5x10^6 cells) group (Fig. 6C). Among the administration methods, intraperitoneal injection markedly outperformed the in-site injection and intravenous tail-vein injection groups in terms of offspring count (P<0.05). However, these numbers remained significantly lower compared with those of the normal group (Fig. 6B). The high-dose (5.0x10^6 cells) and the middle-dose (1.0x10^6 cells) groups produced similar reproductive outcomes, but were both significantly lower compared with the average number of pups in the normal group (P<0.05; Fig. 6C). Collectively, these results suggest that the treatment with UCMSCs could partly restore fertility in rats afflicted with IUA.

Discussion

The limited efficacy of surgical and pharmacological therapies that are currently in practice for the treatment of moderate-to-severe IUAs has necessitated the exploration of regenerative medicine, with stem cell therapy emerging as a promising alternative (20). Among the various stem cell sources, human UCMSCs have been increasingly utilized in clinical trials due to their potent regenerative capabilities and low immunogenicity (8). The present study has highlighted the therapeutic potential of UCMSCs for treating IUAs, with particular focus on both the effectiveness of injecting different concentrations of UCMSCs and the type of delivery route applied. The findings obtained have suggest that UCMSCs can significantly enhance endometrial repair, especially at

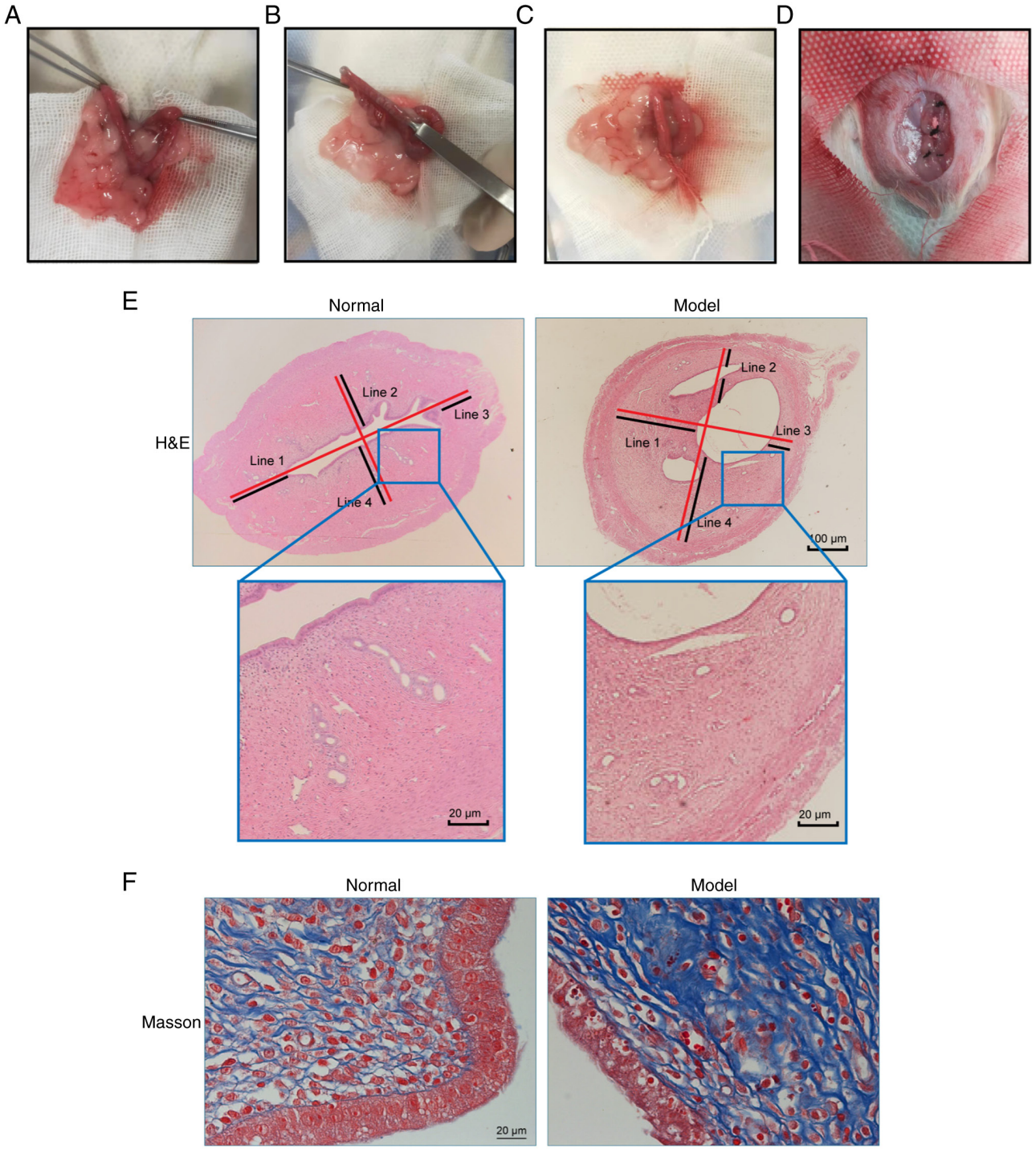

Figure 3. Establishment of the IUA rat model and further histological assessment. Surgical procedure steps for IUA model establishment in rats are shown. (A) Initial surgical exposure of the uterus, (B) mechanical injury applied to the uterine horn, (C) application of an inflammatory agent and (D) post-procedure closure, illustrating the sutured sites. (E) Histological comparison of normal and IUA model uterine tissues. H&E staining was used to show reduced endometrial thickness in the model group compared with that in the normal group. (F) Masson's trichrome staining was used to highlight the increased extent of fibrosis in the model compared with that in the normal group. IUA, intrauterine adhesion.

the optimal dose (found to be $1x10^6$ cells), which consistently outperformed both the lower and the higher doses of UCMSCs in terms of endometrial thickness restoration and fibrosis reduction.

The specific underlying mechanism through which MSCs can promote endometrial repair remains controversial. However, discussions are ongoing regarding whether their regenerative potential stems primarily from their differentiation capabilities or from their secretory functions (21). Evidence supports the hypothesis that the paracrine effects of MSCs serve a predominant role in tissue repair (21). The potential mechanisms through which MSCs facilitate endometrial regeneration in IUA include the following: i) Homing of MSCs to the injury site, followed by differentiation into new endometrial cells; ii) inhibition of epithelial-mesenchymal transition, thereby suppressing the progression of fibrosis;

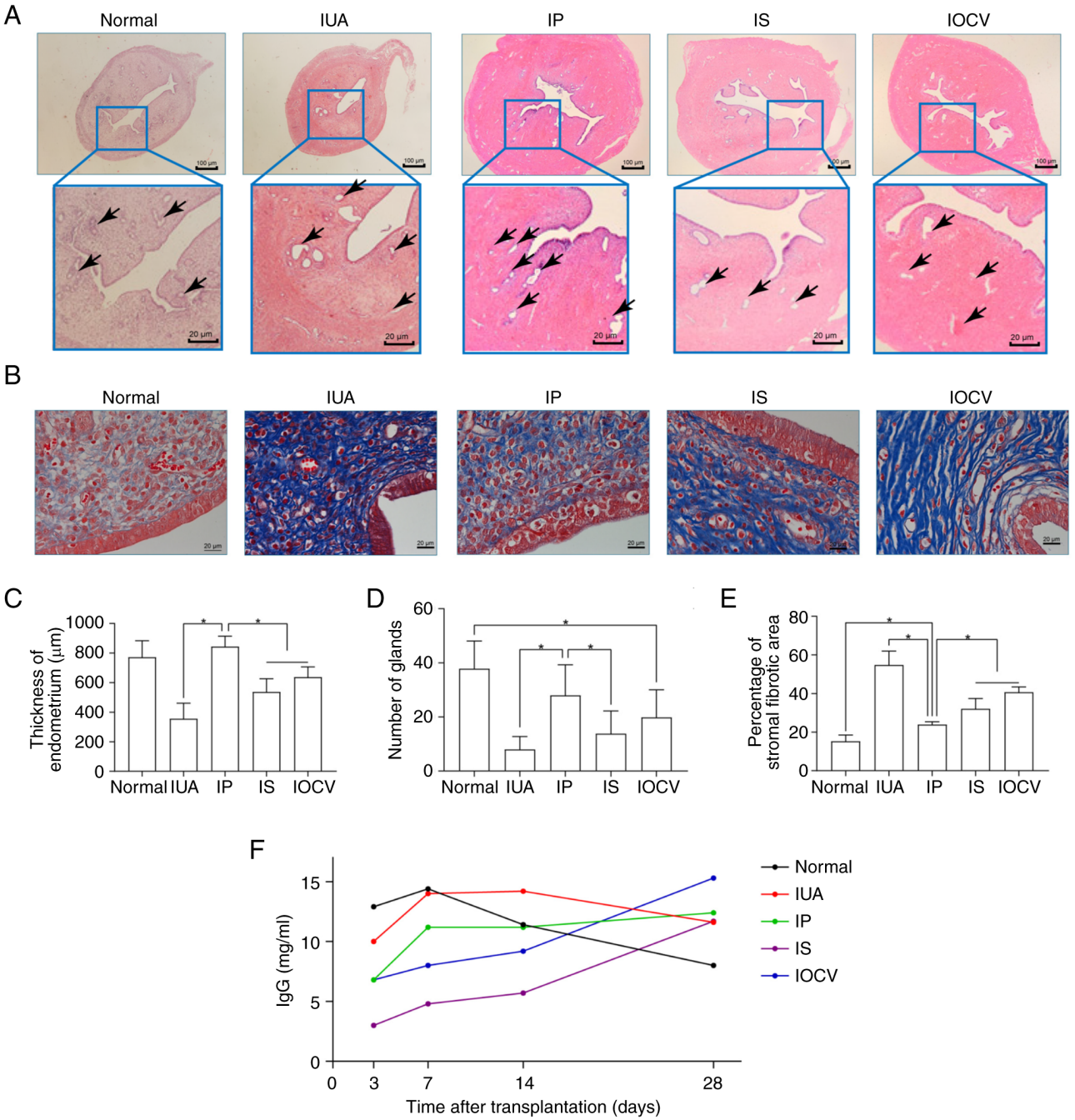

Figure 4. Histological and immunological evaluation of the effectiveness of human umbilical cord-derived mesenchymal stem cell treatment in a rat model of IUA. (A) H&E-stained sections, displaying endometrial thickness among the different experimental groups, namely the normal, IUA, IP, IS and IOCV groups (arrows indicate the endometrial glands). Scale bars represent 100 and 50 μm for the larger and smaller bars, respectively. (B) Masson's trichrome staining highlighting fibrotic areas in the same groups, illustrating variations in fibrosis. (C) A bar graph comparing endometrial thickness among the groups, showing the significantly thicker endometrium in the IP group compared with the IS and IOCV group. (D) A bar graph of the endometrial gland numbers, indicating a higher gland density in the IP group close to normal levels. (E) The percentages of fibrotic areas quantified are shown, with the IP group showing the least fibrosis compared with the other treated and IUA groups. (F) A line graph of IgG levels over time post-transplantation, with the distinct immunological responses among groups highlighted. The IP group's levels initially surged and then stabilized, whereas the IS and IOCV groups showed gradual increases. IUA, intrauterine adhesion; IP, intraperitoneal; IS, intrauterine site injection; IOCV, intravenous ovary-cervix. Data are presented as the mean ± SD. *P<0.05.

iii) regulation of local MSC proliferation and migration to promote endometrial regeneration; iv) release of immunomodulatory factors that can influence angiogenesis; and v) modulation of the immune response through the upregulation of anti-inflammatory cytokines and downregulation of pro-inflammatory cytokines (21,22). However, at present, the clinical translational potential of UCMSCs for IUA treatment remains unclear due to the significant variability in outcomes reported. This was reportedly attributable to various factors, such as cell source, timing of implantation, route of administration and dosage (20). In addition, previous studies have indicated that optimizing these parameters will likely enhance the efficacy of stem cell therapies in restoring uterine function (23,24). The present study has therefore systematically

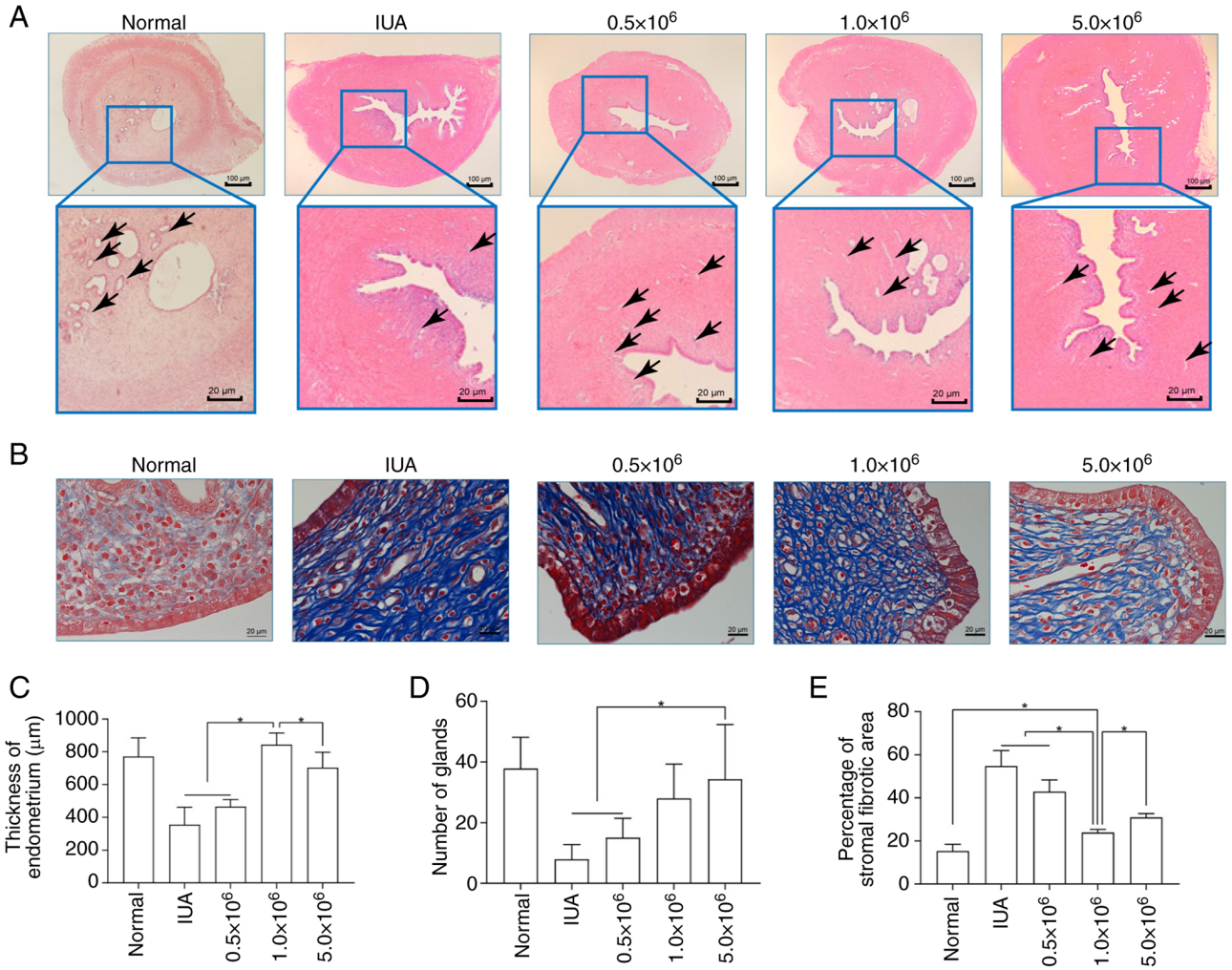

Figure 5. Evaluation of UCMSC therapy in an IUA rat model using various concentrations of UCMSCs. (A) H&E-stained sections, showing endometrial thickness across the treatment groups, namely the Normal, IUA and three UCMSC-dosage ($0.5x10^6$, $1.0x10^6$ and $5.0x10^6$) groups (arrows indicate the glands). Scale bars, 100 and 20 μm. (B) Masson's trichrome staining highlighting differences in the fibrotic area among the same groups. (C) A graph of endometrial thickness, illustrating the significant thickness recovery in the $1.0x10^6$ group, which was approaching that of the normal levels. (D) A bar graph depicting the number of glands, with the $5.0x10^6$ group showing enhanced glandular recovery compared with the other treatment groups. (E) Percentages of the quantified fibrotic areas are shown, indicating the lowest level of fibrosis in the $1.0x10^6$ group, which significantly outperformed the other groups. UCMSCs, human umbilical cord-derived mesenchymal stem cells; IUA, intrauterine adhesion. Data are presented as the mean ± SD. $^*P<0.05$.

evaluated the impact of cell dosage and administration routes on the therapeutic outcomes in a rat model of IUA, emphasizing the importance of precise standardization in preclinical studies to optimize UCMSC treatment protocols for future clinical applications in reproductive disorders, such as IUAs.

UCMSCs have emerged as a promising MSC type for the treatment of endometrial disorders. *In vitro* studies have previously demonstrated that UCMSCs can significantly enhance the proliferation of endometrial stromal cells and promote the expression of vascular markers, contributing to tissue regeneration. Sun *et al* (10) demonstrated that circular RNA (hsa_circRNA_0111659) is upregulated during endometrial repair by UCMSCs, providing a novel perspective on the role of non-coding RNAs in regulating stem cell-mediated repair mechanisms. Similarly, Shi *et al* (25) showed that treatment with UCMSCs led to a significant improvement in the proliferation and angiogenesis of endometrial stromal cells, further highlighting their therapeutic potential. In terms of *in vivo* animal models of IUA, a previous study showed that the administration of UCMSCs during the chronic phase of endometrial injury both facilitated endometrial regeneration and restored fertility in rats (11). Furthermore, another group reported that UCMSCs, through the upregulation of microRNA-455-5p, could enhance endometrial regeneration by modulating the JAK/STAT signaling pathway (12). Collectively, these studies underscored the potential of UCMSC-based therapy for treating IUAs, highlighting the need for further research into optimizing the mode of delivery.

Additionally, the route of UCMSC administration appears to occupy a crucial role in therapeutic outcomes. In animal studies, the local administration of UCMSCs through collagen scaffolds or hydrogels has been shown to improve endometrial regeneration and decrease the extent of fibrosis, whilst collagen scaffolds loaded with UCMSCs have also demonstrated significant benefits in terms of fertility restoration (26,27). Similarly, intraperitoneal, intrauterine and intravenous injections of UCMSCs have all been evaluated, with varying results, depending on the delivery method. Sabry *et al* (28)

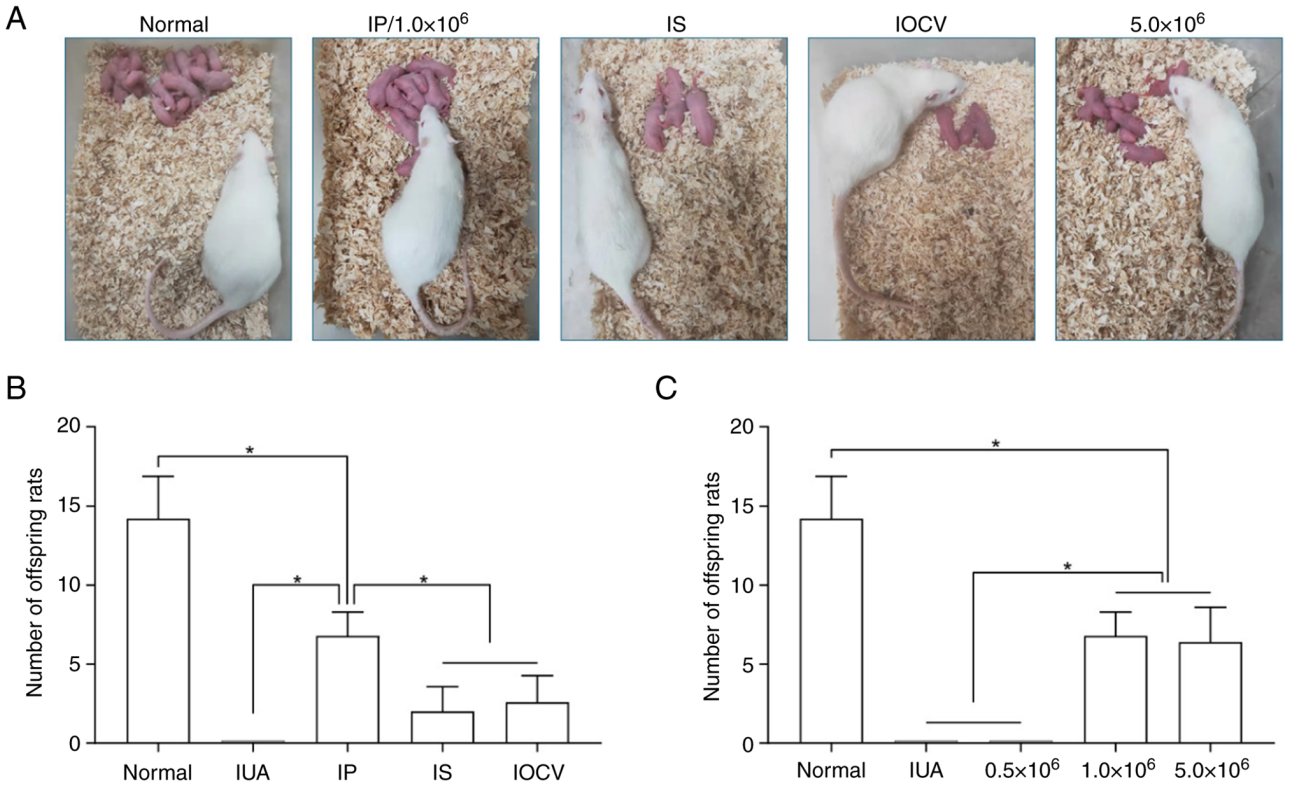

Figure 6. Fertility restoration in an IUA rat model using UCMSC therapy. (A) Visual representation of co-housing experiments with the Normal, IP/1.0x10^6 (intraperitoneal injection of 1.0x10^6 cells), IS, IOCV and 5.0x10^6 cells groups is shown. (B) The numbers of offspring in the Normal, IUA model and different administration route (IP, IS and IOCV) groups are shown. The IP route showed the highest offspring count among the various treatment groups, although it remained lower compared with that in the Normal group. (C) Comparison of offspring numbers among the cell dosage groups (0.5x10^6, 1.0x10^6 and 5.0x10^6 cells), demonstrating that a higher dose does not significantly increase fertility restoration compared with the medium (1.0x10^6 cells) dose, while all were below the Normal group outcomes. The data are shown as the mean ± SD (*P<0.05). The data shown are representative of five independent experiments in each group. IUA, intrauterine adhesion; IP, intraperitoneal; IS, intrauterine site injection; IOCV, intravenous ovary-cervix.

previously showed that combining MSC therapy with neupogen, a granulocyte colony-stimulating factor, resulted in significant improvements in endometrial fibrosis and tissue regeneration, especially when the MSCs were administered intraperitoneally. In another study, the combination of intravenous and intrauterine UCMSC transplantation resulted in superior outcomes compared with intravenous administration alone (29). Although the optimal delivery route for UCMSC therapy remains controversial, several studies have highlighted the need to tailor the approach to the specific characteristics of the target tissue. A previous study on MSC administration for treating type 1 diabetes suggested that the intraperitoneal delivery route was more effective compared with systemic administration in animal models (30). Similarly, studies comparing the efficacy of different administration routes for the MSC-based treatment of colitis found that intravenous administration yielded improved outcomes compared with intraperitoneal delivery in terms of reducing inflammation (31,32). In addition, Zhao *et al* (18) demonstrated that MSC treatment through the intraperitoneal and intrauterine routes was more effective in treating recurrent spontaneous abortion in mice compared with the route of intravenous administration. In clinical settings, the application of UCMSCs through various routes, including the intrauterine and intravenous routes, has shown promise in improving outcomes in patients with Asherman's syndrome or IUAs (11,33-35). Clinical trials have demonstrated that delivering UCMSCs into the uterine cavity, especially when loaded onto a collagen scaffold, is a safe and effective method for improving endometrial regeneration and fertility in patients with recurrent IUAs following adhesiolysis surgery (36,37). In summary, optimizing the delivery route, dosage and integration of biomaterials in UCMSC therapy has been shown to be key in terms of enhancing MSC homing and retention in the endometrium, thereby improving the treatment efficacy for IUAs and advancing the clinical application of UCMSC therapy.

The homing mechanism of MSCs exerts a critical role in tissue regeneration by enabling the recruitment and targeting of stem cells to damaged tissues in need of repair (38). MSC homing can occur through both systemic and site-specific pathways. Systemic homing involves the migration of cells through the bloodstream, extravasation near the lesion and interstitial migration towards the injury site (39). By contrast, non-systemic homing involves local recruitment or the transplantation of MSCs close to the target tissue, where the cells migrate in response to chemokines released from injured tissues. However, the efficiency of MSC homing is typically poor, with <10% of the cells reaching the target site, especially when the MSCs are administered intravenously, since they may become trapped in the lungs (40). Therefore, optimizing the route of administration, whether systemic or non-systemic, has become a crucial factor in improving therapeutic outcomes.

The simplest and most intuitive methods to enhance MSC homing has been proposed to be to deliver the cells directly to or near the target tissue, rather than relying on traditional intravenous infusion (41). By applying the method of localized (non-systemic) administration, MSC retention in the target tissue is likely to improve compared with systemic delivery methods (42). Nevertheless, recent evidence has suggested that the route of administration serves a crucial role in the effectiveness of the treatment, which this is likely to be due to enhanced homing efficiency (41,43). However, to date, to the best of our knowledge, few studies have directly compared targeted with systemic administration, where the majority of the evidence currently available is from meta-analyses (44,45). In the limited comparative studies available, it was observed that the optimal route of MSC administration varies depending on the disease being treated and the characteristics of the target tissue (46-49). Therefore, it is imperative to select the most appropriate MSC delivery method based on the specific attributes of the disease and the target tissue for effective treatment.

In the present study, systemic homing (through tail vein injection) was systematically compared with non-systemic homing (through intraperitoneal and intrauterine wall injections). The results obtained revealed that intraperitoneal injection as the administration route provided the optimal therapeutic outcomes for treating IUAs, most likely due to reduced MSC clearance in the lungs compared with tail-vein injection, which resulted in lower retention of MSCs at the target site. Although intrauterine wall injection represents a targeted approach, it may cause local trauma to the endometrial tissue, thereby hindering the repair process. By contrast, intraperitoneal injection may enhance the homing of UCMSCs to the injured endometrial stroma through the gradient induction of multiple chemotactic factors. These factors include growth factors such as platelet-derived growth factor-AB, insulin-like growth factor-1 and to a lesser extent, chemokines, such as RANTES (also known as chemokine ligand 5), macrophage-derived chemokine and stromal cell-derived factor 1 [also known as C-X-C motif ligand 12 (CXCL12)] (50). Data from a previous study showed that the CM-Dil-labeled cells in the stroma region are significantly higher compared with those in the superficial myometrium, in the seroma and in the epithelium. Along with the CM-Dil-labeled UCMSC tracking experiments in the present study, confirmed that intraperitoneally administered UCMSCs can home to the endometrial stroma (17).

The present study also focused on investigating the routes of administration and dosages of UCMSC therapy for treating IUAs, with a preliminary exploration of the therapeutic effects of systemic compared with non-systemic homing. Future clinical practices could enhance MSC homing efficiency through a number of possible methods, such as genetic modification, cell surface modulation, *in vitro* priming of MSCs, reducing intravascular trapping in the lungs, and utilizing chemokine- or cytokine-impregnated hydrogel scaffolds, nanoparticle-based chemokine release (such as using CXCL12) or pulsed ultrasound targeting injured tissues. To avoid the influence of scaffold materials on the effect of UCMSCs, the present study did not include intrauterine infusion, a commonly used administration route. However, intrauterine infusion or placement of biomaterials loaded with MSCs may represent the optimal future approach for UCMSC therapy in IUA treatment. Although MSCs may be potentially applied in reproductive medicine, their procurement can require invasive procedures, especially in the case of bone marrow MScs (BMMSCs), which has higher risk of tumorigenesis and immunoreactivity (51). The paradigm of biomedical research is shifting towards developing personalized therapies. Future therapeutic strategies may consist of combinations of stem cell-based therapies that promote cell renewal and differentiation, and acellular therapies that modulate inflammation and promote tissue repair, coupled with biomaterials that concentrate these actions at the target site. These synergistic approaches could hold the key to restoring endometrial function, ultimately improving reproductive outcomes for patients with uterine-factor infertility. On the basis of the existing evidence concerning the cost, accessibility and availability of the therapies discussed herein, a 'triple-hit' regenerative strategy has been proposed, which would combine high-yield MSCs (such as BMMSCs or UCMSCs) with acellular treatments, possibly integrated into extracellular matrix hydrogels (20). Considered individually, these approaches have demonstrated efficacy, but their combined impact may yet significantly transform the clinical management of endometrial disorders once their synergistic effects have been verified. Finally, multi-center randomized controlled trials are essential to further evaluate the safety and efficacy of these biotechnological treatments.

In conclusion, the present study has demonstrated the significant therapeutic potential of UCMSCs for treating IUAs, especially emphasizing the superior efficacy of an optimal dose of $1x10^6$ cells and the intraperitoneal delivery route in terms of enhancing endometrial repair by restoring endometrial thickness and reducing fibrosis. These findings underscore the importance of dosage and delivery route optimization for maximizing the therapeutic benefits of UCMSCs in IUA treatment.

Acknowledgements

Not applicable.

Funding

The present study was supported by the Innovative Capacity Improvement Plan of Hebei Province (S&T Program of Hebei; grant no. 20577705D).

Availability of data and materials

The data generated in the present study may be requested from the corresponding author.

Authors' contributions

MLZ, ZKL and XHH provided the concept and design for this study. HG, JHZ and YPT conducted the experiments and wrote the manuscript. YLX, QL and YFD were responsible for the identification of mesenchymal stem cells. MLZ and HG were

responsible for data analysis and preparing the figures. ZKL, MLZ and XHH discussed and revised the manuscript. XHH and ZKL reviewed the manuscript. All authors agree to the submission and publication of the final manuscript. MLZ and HG confirm the authenticity of all the raw data. All authors have read and approved the manuscript.

Ethics approval and consent to participate

The design and implementation steps of the animal experiments, as well as the acquisition of human umbilical cords, were approved by the Institution Animal Ethics Committee of the Second Hospital of Hebei Medical University (Shijiazhuang, China; approval no. 2020-R285; approval no. for animal study: 2021-AE261). Written informed consent was obtained from the mothers who donated the umbilical cords for research purposes.

Patient consent for publication

Not applicable.

Competing interests

The authors declare that they have no competing interests.

References

1. Ma J, Zhan H, Li W, Zhang L, Yun F, Wu R, Lin J and Li Y: Recent trends in therapeutic strategies for repairing endometrial tissue in intrauterine adhesion. Biomater Res 25: 40, 2021.
2. Hooker AB, Lemmers M, Thurkow AL, Heymans MW, Opmeer BC, Brölmann HA, Mol BW and Huirne JA: Systematic review and meta-analysis of intrauterine adhesions after miscarriage: prevalence, risk factors and long-term reproductive outcome. Hum Reprod Update 20: 262-278, 2014.
3. Hooker AB, De Leeuw RA, Emanuel MH, Mijatovic V, Brolmann HAM and Huirne JAF: The link between intrauterine adhesions and impaired reproductive performance: A systematic review of the literature. BMC Pregnancy Childbirth 22: 837, 2022.
4. Tu CH, Yang XL, Qin XY, Cai LP and Zhang P: Management of intrauterine adhesions: A novel intrauterine device. Med Hypotheses 81: 394-396, 2013.
5. Han Y, Li X, Zhang Y, Han Y, Chang F and Ding J: Mesenchymal Stem cells for regenerative medicine. Cells 8: 886, 2019.
6. Pittenger MF, Mackay AM, Beck SC, Jaiswal RK, Douglas R, Mosca JD, Moorman MA, Simonetti DW, Craig S and Marshak DR: Multilineage potential of adult human mesenchymal stem cells. Science 284: 143-147, 1999.
7. Ma J, Wu J, Han L, Jiang X, Yan L, Hao J and Wang H: Comparative analysis of mesenchymal stem cells derived from amniotic membrane, umbilical cord, and chorionic plate under serum-free condition. Stem Cell Res Ther 10: 19, 2019.
8. El Omar R, Beroud J, Stoltz JF, Menu P, Velot E and Decot V: Umbilical cord mesenchymal stem cells: the new gold standard for mesenchymal stem cell-based therapies?. Tissue Eng Part B Rev 20: 523-544, 2014.
9. Yang X, Zhang M, Zhang Y, Li W and Yang B: Mesenchymal stem cells derived from Wharton jelly of the human umbilical cord ameliorate damage to human endometrial stromal cells. Fertil Steril 96: 1029-1036, 2011.
10. Sun B, Shi L, Shi Q, Jiang Y, Su Z, Yang X and Zhang Y: Circular RNAs are abundantly expressed and upregulated during repair of the damaged endometrium by Wharton's jelly-derived mesenchymal stem cells. Stem Cell Res Ther 9: 314, 2018.
11. Zhang L, Li Y, Guan CY, Tian S, Lv XD, Li JH, Ma X and Xia HF: Therapeutic effect of human umbilical cord-derived mesenchymal stem cells on injured rat endometrium during its chronic phase. Stem Cell Res Ther 9: 36, 2018.
12. Sun D, Jiang Z, Chen Y, Shang D, Miao P and Gao J: MiR-455-5p upregulation in umbilical cord mesenchymal stem cells attenuates endometrial injury and promotes repair of damaged endometrium via Janus kinase/signal transducer and activator of transcription 3 signaling. Bioengineered 12: 12891-12904, 2021.
13. Wang L, Yu C, Chang T, Zhang M, Song S, Xiong C, Su P and Xiang W: In situ repair abilities of human umbilical cord-derived mesenchymal stem cells and autocrosslinked hyaluronic acid gel complex in rhesus monkeys with intrauterine adhesion. Sci Adv 6: eaba6357, 2020.
14. Giri J and Galipeau J: Mesenchymal stromal cell therapeutic potency is dependent upon viability, route of delivery, and immune match. Blood Adv 4: 1987-1997, 2020.
15. Levy O, Kuai R, Siren EMJ, Bhere D, Milton Y, Nissar N, De Biasio M, Heinelt M, Reeve B, Abdi R, *et al*: Shattering barriers toward clinically meaningful MSC therapies. Sci Adv 6: eaba6884, 2020.
16. Dominici M, Le Blanc K, Mueller I, Slaper-Cortenbach I, Marini F, Krause D, Deans R, Keating A, Prockop Dj and Horwitz E: Minimal criteria for defining multipotent mesenchymal stromal cells. The International Society for Cellular Therapy position statement. Cytotherapy 8: 315-317, 2006.
17. Zheng JH, Zhang JK, Kong DS, Song YB, Zhao SD, Qi WB, Li YN, Zhang ML and Huang XH: Quantification of the CM-Dil-labeled human umbilical cord mesenchymal stem cells migrated to the dual injured uterus in SD rat. Stem Cell Res Ther 11: 280, 2020.
18. Zhao S, Qi W, Zheng J, Tian Y, Qi X, Kong D, Zhang J and Huang X: Exosomes derived from adipose mesenchymal stem cells restore functional endometrium in a rat model of intrauterine adhesions. Reprod Sci 27: 1266-1275, 2020.
19. Kong D, Zhang L, Xu X, Zhang J, Li Y and Huang X: Small intestine submucosa is a potential material for intrauterine adhesions treatment in a rat model. Gynecol Obstet Invest 83: 499-507, 2018.
20. Rodríguez-Eguren A, Bueno-Fernandez C, Gómez-Álvarez M, Francés-Herrero E, Pellicer A, Bellver J, Seli E and Cervelló I: Evolution of biotechnological advances and regenerative therapies for endometrial disorders: A systematic review. Hum Reprod Update 30: 584-613, 2024.
21. Azizi R, Aghebati-Maleki L, Nouri M, Marofi F, Negargar S and Yousefi M: Stem cell therapy in Asherman syndrome and thin endometrium: Stem cell-based therapy. Biomed Pharmacother 102: 333-343, 2018.
22. Guo LP, Chen LM, Chen F, Jiang NH and Sui L: Smad signaling coincides with epithelial-mesenchymal transition in a rat model of intrauterine adhesion. Am J Transl Res 11: 4726-4737, 2019.
23. Arikan G, Turan V, Kurekeken M, Goksoy HS and Dogusan Z: Autologous bone marrow-derived nucleated cell (aBMNC) transplantation improves endometrial function in patients with refractory Asherman's syndrome or with thin and dysfunctional endome-trium. J Assist Reprod Genet 40: 1163-1171, 2023.
24. de Miguel-Gómez L, López-Martínez S, Campo H, Francés-Herrero E, Faus A, Díaz A, Pellicer A, Domínguez F and Cervelló I: Comparison of different sources of platelet-rich plasma as treatment option for infertility-causing endometrial pathologies. Fertil Steril 115: 490-500, 2021.
25. Shi Q, Sun B, Wang D, Zhu Y, Zhao X, Yang X and Zhang Y: Circ6401, a novel circular RNA, is implicated in repair of the damaged endometrium by Wharton's jelly-derived mesenchymal stem cells through regulation of the miR-29b-1-5p/RAP1B axis. Stem Cell Res Ther 11: 520, 2020.
26. Xin L, Lin X, Pan Y, Zheng X, Shi L, Zhang Y, Ma L, Gao C and Zhang S: A collagen scaffold loaded with human umbilical cord-derived mesenchymal stem cells facilitates endometrial regeneration and restores fertility. Acta Biomater 92: 160-171, 2019.
27. Liu Y, Cai J, Luo X, Wen H and Luo Y: Collagen scaffold with human umbilical cord mesenchymal stem cells remarkably improves intrauterine adhesions in a rat model. Gynecol Obstet Invest 85: 267-276, 2020.
28. Sabry D, Mostafa A, Marzouk S, Ibrahim W, Ali HHM, Hassan A and Shamaa A: Neupogen and mesenchymal stem cells are the novel therapeutic agents in regeneration of induced endometrial fibrosis in experimental rats. Biosci Rep 37: BSR20170794, 2017.
29. Zhuang M, Zhang W, Cheng N, Zhou L, Liu D, Yan H, Fang G, Heng BC, Sun Y and Tong G: Human umbilical cord mesenchymal stromal cells promote the regeneration of severe endometrial damage in a rat model. Acta Biochim Biophys Sin (Shanghai) 54: 148-151, 2022.

30. Hashemi SM, Hassan ZM, Hossein-Khannazer N, Pourfathollah AA and Soudi S: Investigating the route of administration and efficacy of adipose tissue-derived mesenchymal stem cells and conditioned medium in type 1 diabetic mice. Inflammopharmacology 28: 585-601, 2020.
31. Goncalves Fda C, Schneider N, Pinto FO, Meyer FS, Visioli F, Pfaffenseller B, Lopez PL, Passos EP, Cirne-Lima EO, Meurer L and Paz AH: Intravenous vs intraperitoneal mesenchymal stem cells administration: What is the best route for treating experimental colitis?. World J Gastroenterol 20: 18228-18239, 2014.
32. Huldani H, Margiana R, Ahmad F, Opulencia MJC, Ansari MJ, Bokov DO, Abdullaeva NN and Siahmansouri H: Immunotherapy of inflammatory bowel disease (IBD) through mesenchymal stem cells. Int Immunopharmacol 107: 108698, 2022.
33. Zhou S, Lei Y, Wang P, Chen J, Zeng L, Qu T, Maldonado M, Huang J, Han T, Wen Z, *et al*: Human umbilical cord mesenchymal stem cells encapsulated with pluronic F-127 enhance the regeneration and angiogenesis of thin endometrium in rat via local IL-1β stimulation. Stem Cells Int 2022: 7819234, 2022.
34. Wang H, Yang X, Chen X, Xie H, Wang J and Zhang Y: Identify the role of human Wharton's jelly mesenchymal stem cells in repairing injured uterine of rat. J Obstet Gynaecol Res 47: 320-328, 2021.
35. Zhang L, Li Y, Dong YC, Guan CY, Tian S, Lv XD, Li JH, Su X, Xia HF and Ma X: Transplantation of umbilical cord-derived mesenchymal stem cells promotes the recovery of thin endometrium in rats. Sci Rep 12: 412, 2022.
36. Cao Y, Sun H, Zhu H, Zhu X, Tang X, Yan G, Wang J, Bai D, Wang J, Wang L, *et al*: Allogeneic cell therapy using umbilical cord MSCs on collagen scaffolds for patients with recurrent uterine adhesion: A phase I clinical trial. Stem Cell Res Ther 9: 192, 2018.
37. Kaczynski JB and Rzepka JK: Endometrial regeneration in Asherman's syndrome and endometrial atrophy using Wharton's jelly-derived mesenchymal stem cells. Ginekol Pol 93: 904-909, 2022.
38. Liesveld JL, Sharma N and Aljitawi OS: Stem cell homing: From physiology to therapeutics. Stem Cells 38: 1241-1253, 2020.
39. Nitzsche F, Muller C, Lukomska B, Jolkkonen J, Deten A and Boltze J: Concise review: MSC adhesion cascade-insights into homing and transendothelial migration. Stem Cells 35: 1446-1460, 2017.
40. Krueger TEG, Thorek DLJ, Denmeade SR, Isaacs JT and Brennen WN: Concise review: Mesenchymal stem cell-based drug delivery: The good, the bad, the ugly, and the promise. Stem Cells Transl Med 7: 651-663, 2018.
41. Yuan M, Hu X, Yao L, Jiang Y and Li L: Mesenchymal stem cell homing to improve therapeutic efficacy in liver disease. Stem Cell Res Ther 13: 179, 2022.
42. Ullah M, Liu DD and Thakor AS: Mesenchymal stromal cell homing: Mechanisms and strategies for improvement. iScience 15: 421-438, 2019.
43. Maric DM, Velikic G, Maric DL, Supic G, Vojvodic D, Petric V and Abazovic D: Stem cell homing in intrathecal applications and inspirations for improvement paths. Int J Mol Sci 23: 4290, 2022.
44. Jiang Z, Chen L, Huang L, Yu S, Lin J, Li M, Gao Y and Yang L: Bioactive materials that promote the homing of endogenous mesenchymal stem cells to improve wound healing. Int J Nanomedicine 19: 7751-7773, 2024.
45. Liu Z, Mikrani R, Zubair HM, Taleb A, Naveed M, Baig MMFA, Zhang Q, Li C, Habib M, Cui X, *et al*: Systemic and local delivery of mesenchymal stem cells for heart renovation: Challenges and innovations. Eur J Pharmacol 876: 173049, 2020.
46. Kanelidis AJ, Premer C, Lopez J, Balkan W and Hare JM: Route of delivery modulates the efficacy of mesenchymal stem cell therapy for myocardial infarction: A meta-analysis of preclinical studies and clinical trials. Circ Res 120: 1139-1150, 2017.
47. Jeong H, Yim HW, Park HJ, Cho Y, Hong H, Kim NJ and Oh IH: Mesenchymal stem cell therapy for ischemic heart disease: Systematic review and meta-analysis. Int J Stem Cells 11: 1-12, 2018.
48. Peng W, Sun J, Sheng C, Wang Z, Wang Y, Zhang C and Fan R: Systematic review and meta-analysis of efficacy of mesenchymal stem cells on locomotor recovery in animal models of traumatic brain injury. Stem Cell Res Ther 6: 47, 2015.
49. Augustine S, Avey MT, Harrison B, Locke T, Ghannad M, Moher D and Thébaud B: Mesenchymal stromal cell therapy in bronchopulmonary dysplasia: Systematic review and meta-analysis of preclinical studies. Stem Cells Transl Med 6: 2079-2093, 2017.
50. Ponte AL, Marais E, Gallay N, Langonné A, Delorme B, Hérault O, Charbord P and Domenech J: The in vitro migration capacity of human bone marrow mesenchymal stem cells: Comparison of chemokine and growth factor chemotactic activities. Stem Cells 25: 1737-1745, 2007.
51. Ramaswamy Reddy SH, Reddy R, Babu NC and Ashok GN: Stem-cell therapy and platelet-rich plasma in regenerative medicines: A review on pros and cons of the technologies. J Oral Maxillofac Pathol 22: 367-374, 2018.